COMMUNICATION

Tetracationic Cobalt 3,4-pyridinoporphyrazine for Direct CO_2 to Methanol Conversion Escaping the CO Intermediate Pathway

Chanjuan Zhang, [a]⊥ Jorge Follana-Berná, [b] Diana Dragoe,[a] Zakaria Halime,[a] Philipp Gotico,[c] Ángela Sastre-Santos,[b],* and Ally Aukauloo [a,c],*

[a] Dr. C. Zhang, Dr. D. Dragoe, Dr. Z. Halime, Prof. A. Aukauloo
Université Paris-Saclay, CNRS, Institut de Chimie Moléculaire et des Matériaux d'Orsay, 91405, Orsay, France.
E-mail: ally.aukauloo@universite-paris-saclay.fr
⊥ Dr. C. Zhang
Current address: Electrochemical Excellent Center, Flemish Institute for Technological Research (VITO), Boeretang 200, 2400 Mol, Belgium
[b] Dr. Jorge Follana-Berná and Prof. Ángela Sastre-Santos
Área de Química Orgánica, Instituto de Bioingeniería
Universidad Miguel Hernández
Avda. de la Universidad s/n 03203 Elche, Spain
E-mail: asastre@umh.es
[c] Dr. P. Gotico, Prof. A. Aukauloo
Institute for Integrative Biology of the Cell, CEA, CNRS, Université Paris-Saclay
91191 Gif-sur-Yvette (France)

Supporting information for this article is given via a link at the end of the document.

Abstract: Molecular catalysts offer a unique opportunity to implement different chemical functionalities to steer the efficiency and selectivity for the CO_2 reduction for instance. Metalloporphyrins and metallophthalocyanines are under high scrutiny since their most classic derivatives the tetraphenylporphyrin (TPP) and parent phthalocyanine (Pc), have been used as the molecular platform to install, hydrogen bonds donors, proton relays, cationic fragments, incorporation in MOFs and COFs, to enhance the catalytic power of these catalysts. Herein, we examine the electrocatalytic properties of the cobalt (II) tetramethyl tetrapyridinoporphyrazine (**CoTmTPyPz**) for the reduction of CO_2 in heterogeneous medium when adsorbed on carbon nanotubes (CNT) at a carbon paper (CP) electrode. Unlike reported electrocatalysis with cobalt based phthalocyanine where CO was advocated as the two electron and two protons reduced intermediate on the way to the formation of methanol, we found here that **CoTmTPyPz** does not reduce CO to methanol. Henceforth, ruling out a mechanistic pathway where CO is a reaction intermediate.

Using renewable energy sources to convert CO_2 into energy dense compounds is a privilege pathway towards developing a sustainable world.[1] The journey towards an extensive industrial process is still not a short-term scenario. Much work is yet needed in the design of catalysts both in solid states and molecular fields to reach these goals.[1b, 1d, 2] Solid state catalysts often lead to the formation of single to multiple carbon atoms molecules.[1g, 3] It is therefore imperative to steer the reactivities of catalysts towards a desired reduced form of CO_2. Molecular catalysis distinguishes itself through the versatile synthesis of ligand sets to interrogate the structure-reactivity relationship. However, a still unresolved challenge concerns the selectivity of the targeted products. In the molecular approach, chemists are developing bioinspired synthetic models where chemical features in the first and second coordination spheres of the active metal sites of enzymes are being introduced in the ligand scaffolds to shape the reactivity of the first-row transition elements.[1d, 1g, 2b-e, 3d, 4] In the plethora of molecular catalysts that have been developed recently, metalloporphyrins and metallophthalocyanines have been recognized as stable and efficient catalysts for the CO_2 reduction.[5] To date, the grand majority of these systems have shown a good selectivity for the two-electron and two-proton reduction of CO_2 to CO competing with the easier hydrogen evolution reaction.[6] Interestingly, some of these complexes are able to realize more than the two-electron reduction to yield methanol or methane.[3c, 7] This performance has been realized more widely when the catalysts were immobilized on conductive high surface materials such as carbon nanotubes and other carbonaceous electrodes.[3c, 7a, 7b, 7d] This strategy brings another tuning parameter for the optimization of the catalytic performance of the molecular catalysts. Cobalt phthalocyanine (**CoPc**) a robust complex used in the fabrication of inks, were reported by Jaramillo and Robert and coworkers as being able to electrocatalytically convert CO_2 to methanol with a net yield of 0.3% in a stepwise fashion where CO was proposed as an intermediate on the catalytic route.[5a] The authors have demonstrated that replacing CO_2 by CO under the same catalytic conditions, methanol was also detected. While Wang and collaborators have also reported on the electrocatalytic CO selective reduction to MeOH with **CoPc** as catalyst when adsorbed on carbon CNT/carbon fiber electrode.[7b] Of note, the differing reported Faradaic efficiency values for the parent cobalt (II) phthalocyanine catalyst for the direct CO_2 to MeOH conversion (44 to 0.3 %) could be allocated to the experimental conditions. Further insights in the electrochemical process for the CO_2/CO reduction to methanol came from a recent theoretical study where the authors have proposed that the redox activity of the phthalocyanine ring is playing a crucial role in storing both the electron and protons transferring hydrogen atom to the CO_2 metal bound CO_2.[8] The involvement of the phthalocyanine macrocycle directly in the catalytic steps for the six-electron and six-proton transfer process opens a new pathway model to optimize the reactivity/structure efficacy.

In this study, we have focused on the electrochemical reactivity of the cobalt (II) tetramethyl tetrapyridinoporphyrazine hereafter abbreviated as **CoTmTPyPz** (see Scheme 1) when immobilized on CNT at the surface of a high surface area carbon paper electrode. The choice for this fused tetrapyridinoporphyrazine was motivated by recent studies where cationic functions were shown to play an essential role in the catalytic enhancement metalloporphyrins and phthalocyanines complexes.[2d, 9] Furthermore, we anticipate that the pyridinium functions being electroactive may be the locus for the storage of electrons aside the cobalt ion and the phorphyrazine macrocycle as classical observed. We found here that the **CoTmTPyPz** when adsorbed on a CNT/CP electrode can convert CO_2 directly into MeOH with a Faradaic efficiency (FE) of *ca.* 15% at -1.0 V *vs* RHE and in a CO_2 saturated aqueous solution with 0.5 M $KHCO_3$ used as electrolyte. This result is confronted to the 6.9 % FE found for the parent cobalt (II) phthalocyanine (**CoPc**) catalyst under the same conditions. The electrocatalytic reduction of CO was found to be negligible with the **CoTmTPyPz** catalyst in comparison with the **CoPc**. The presence of the pyridinium groups in the second coordination sphere of the cobalt center may account for this change in mechanistic pathways leading to the formation of MeOH from CO_2.

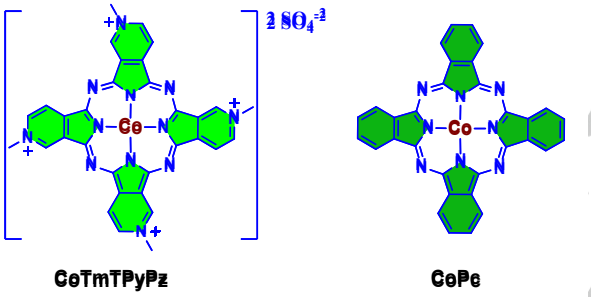

Scheme 1. Chemical structure of tetramethyl cobalt (II) tetrapyridinoporphyrazine (**CoTmTPyPz**) and cobalt (II) phthalocyanine (**CoPc**).

The synthesis of **CoTmTPyPz** was realized following reported procedures [10] and is given in the SI. For simplicity, we represent the isomer with a C_{4h} symmetry. No purification method permitted the isolation of a pure geometrical isomer given the poor solubility of **CoTmTPyPz** in classic organic solvents. Our initial investigation was to study the electrochemical properties of **CoTmTPyPz** using cyclic voltammetry in mQ water with 0.1 M KCl as the supporting electrolyte (Figure S8). Under Ar, **CoTmTPyPz** displayed two quasi-reversible redox peaks at -0.143 V and -0.762 V *vs* NHE, corresponding to the formal $Co^{II/I}$ and $Co^{I/0}$, respectively. Importantly, we noticed that upon cycling several times in the cathodic region that the current intensity increases and reaches a plateau pertaining the deposition of the **CoTmTPyPz** at the surface of the CNT/CP electrode (Figure S9 and S10). Therefore, we reasoned that the deposition of the **CoTmTPyPz** complex at the surface of the electrode would hamper any mechanistic investigation of the CO_2 electroreduction in a homogeneous phase. Taking profit of this ready electro-adsorption of **CoTmTPyPz** we prepared a modified CNT/CP electrode for further study in a heterogeneous medium (see SI for a detailed procedure).

CoPc has been reported as among the short list of molecular catalysts that can reduce CO_2 further than the commonly observed two electron process in particular to MeOH going through a CO intermediate. We initiated our investigation by performing a controlled potential electrolysis in an aqueous solution with the different modified electrodes **CoPc**/CNT/CP and **CoTmTPyPz**/CNT/CP electrodes in a CO-saturated 0.5 M KCl aqueous solution instead of a $KHCO_3$ electrolyte to exclude any possible source of CO_2 (Figure 1). Interestingly, we found that the **CoPc**/CNT/CP electrode was able to convert CO to methanol, but with a selectivity of only 1.3% under our experimental conditions and considering the nature of the modified electrodes. This value

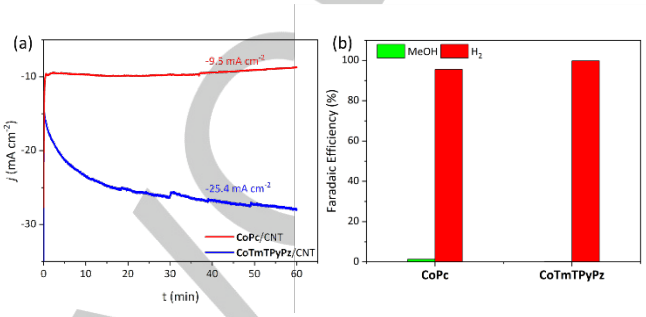

Figure 1. (a) j *vs* t, (b) Faradaic efficiency of methanol (green) and H_2 (red) for the controlled potential electrolysis of **CoPc**/CNT/CP (red) and **CoTmTPyPz**/CNT/CP (blue) electrodes in CO-saturated 0.5 M KCl aqueous solution (catholyte) and 0.5 M $KHCO_3$ aqueous solution was used for the anolyte

is to be compared with 28 % and 0.3 % obtained for the direct reduction of CO to MeOH by Wang *et col.* and Robert *et col.* in presence of $KHCO_3$ and K_2HPO_4 as electrolyte respectively. [5a, 7b] This comparative experiment is important to position the reactivity of our modified electrodes. Interestingly, we found that the electrochemical activity for the **CoTmTPyPz**/CNT/CP electrode for the reduction of CO to MeOH was negligible even in a basic medium (Figure S11). These results clearly reveal that in the case of **CoTmTPyPz**, CO is not the major intermediate to account for the mechanistic route leading to the formation of MeOH. As we can notice in Figure 1, that H_2 evolution reaction was prevailing for both modified electrodes. However, the **CoTmTPyPz** outperforms **CoPc** by more than three-fold with a current density reaching 30 against 9.5 mA cm^{-2} after one hour of electrolysis respectively. This distinctive catalytic properties of **CoTmTPyPz** for the H_2 production in comparison to **CoPc** is also a clear effect of the presence of the fused pyridinium rings on the porphyrazine ring. We anticipate that the pyridinium units may function as charge storage modules working in synergy with the reduced cobalt center to boost the H_2 production. Such an enhancement for the hydrogen production reaction was reported for a series of iron porphyrin derivatives.[11]

We performed a controlled potential electrolysis with the **CoTmTPyPz**/CNT/CP modified electrode in a CO_2-saturated aqueous solution containing 0.1 M $NaHCO_3$ at -1.0 V *vs.* RHE. The electrolysis was conducted for 2 hours and revealed that **CoTmTPyPz**/CNT/CP had a stable and high current density throughout the process. The average current density was *ca.* -4.23 mA.cm^{-2}, indicating a stable continuous CO_2 electrolysis (Figure S12a). Gas product analysis with a micro-GC showed that after 30 minutes of electrolysis, the faradic efficiency of CO_2 to CO conversion was 96.6 % (Figure S12b). The little fall in the CO selectivity to 94.8 % after 2 hours of electrolysis was attributed to the change in the local increase of pH environment, due to the consumption of H^+ or the CO_2 upon the fast electrochemical process. The post **CoTmTPyPz**/CNT/CP was then employed in a fresh electrolyte at the same potential for 2 hours. During the second cycle, the current density was stable, with an average

current density of -5.23 mA.cm^{-2}, which was even slightly greater than that of the first cycle. These results are supportive that the designed **CoTmTPyPz** is an efficient molecular catalyst for CO_2 electroreduction. However, under these experimental conditions, the NMR analysis of the electrolyte did not reveal any trace of liquid products such as formate, formaldehyde, or methanol. At this point, we set to interrogate the electrolyzer configuration for ameliorating the electrochemical performance. For this, we performed different electrolyses in presence of a higher electrolyte concentration (0.5 M $KHCO_3$) of a CO_2-saturated aqueous solution at various potentials (-0.90 V, -0.95 V, -1.0 V, -1.05 V, and -1.10 V *vs.* RHE). The **CoTmTPyPz**/CNT/CP electrode showed stable current densities upon electrolysis within this potential window (Figure S13a). For instance, at -1.0 V *vs* RHE, the current density increases to -23.69 mA cm^{-2}, almost six times higher than that with 0.1 M $NaHCO_3$ (-4.23 mA cm^{-2}), indicating that higher electrolyte concentrations significantly improved the electrocatalytic steps. After one hour of electrolysis, micro-GC and NMR analyses of the gas and liquid products account for a total faradaic efficiency of around 90 % for CO and MeOH at -0.90 V and -0.95 V *vs* RHE (Figure S13b). The selectivity of MeOH increases as the controlled potentials drop from -0.9 V to -1.0 V and reaches a maximum selectivity of 13.7 % with a partial current density of -3.25 mA.cm^{-2} at -1.0 V *vs* RHE (Figure S14). At more negative potentials, the faradaic efficiency of MeOH decreased while the proton reduction was favored. Hence, we chose -1.0 V *vs.* RHE as the optimal potential for further investigation. An isotopic labeling experiment was conducted to confirm that the formation of methanol was indeed originating from the CO_2 electroreduction. This experiment involved injecting partly to a $^{12}CO_2$-saturated 0.5 M $KHCO_3$ aqueous solution with a $^{13}CO_2$ flow for 2 minutes and pursuing electrocatalysis under identical conditions. The ^{1}H NMR spectra (Figure 2 and S15) of the post electrolyte clearly depict in the case when $^{13}CO_2$ was present a split of signal representing the CH_3 proton peak (δ = 3.35 ppm) into a doublet with a coupling constant (J_{HC}) of 142 Hz,[5a] confirming that $^{13}CO_2$ substrate was the source of $^{13}CH_3OH$ formation. The applied spinning speed during all the ^{1}H NMR measurement for the post-electrolyte was set to 0, eliminating the possibility of a spinning side band. This further confirmed that the splitting signal resulted from the coupling between ^{1}H and ^{13}C from the methyl group of $^{13}CH_3OH$.

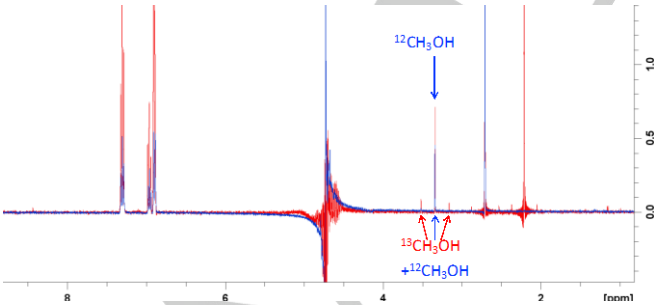

Figure 2. ^{1}H NMR spectra of the electrolyte after controlled potential electrolysis (E = -1.0 V vs RHE, t=2 h) in $^{12}CO_2$-saturated (blue trace) and $^{12}CO_2$-saturated but in presence of $^{13}CO_2$ (red trace) 0.5 M $KHCO_3$ solutions

At this stage, the gathered results confirm that the **CoTmTPyPz**/CNT/CP electrode can directly transform CO_2 to MeOH without CO being a major intermediate in the electrocatalytic cycle. Under these premises, it was important to check for the stability of the cobalt complex at the surface of the CNT. While the total current density remained stable throughout the entire 2-hour electrolysis, the faradaic efficiency of methanol gradually decreased from 13.8 % to 13.7 % at 60 minutes, and ultimately reached the lowest faradaic efficiency of 9.4 % after the 2-hour electrolysis (Figure S16). This decrease can be attributed to the decomposition of **CoTmTPyPz** molecules to form an alternate catalytic metallic system, a decrease of the adsorbed molecular catalyst at the surface of the electrode or modifications in the working conditions of the electrolyte. Of note, the pH of the post-electrolyte increased from the initial 7.2 to 9.3, that may account for the drop in the CO_2 electroreduction and the consequent consumption of protons (six protons for one methanol formation).

Pursuing our effort to investigate the fate of the catalyst at the surface of the electrode after electrocatalysis, we conducted a XPS and UV/vis characterization of the fresh and post electrodes. The resulting XPS survey spectra showed similar peaks for N1s, C1s, and Co2p from **CoTmTPyPz**, K2s, Cl2s, Si2s, and Si2p from the KCl electrolyte and the sintered frit during the "electro-adsorption" process (Figure S17a). Furthermore, the N1s and Co2p core-level spectra are similar for **CoTmTPyPz**/CNT/CP electrode before and after electrolysis (Figure S17b-e). The fitting procedure implied the use of gauss-Lorentz functions with 30% Lorentzian character, after the subtraction of a Shirley-type background. The N1s spectra show two main contributions, located at 399.2 and 400.8 eV and a pi shake-up satellite at 402.5 eV. The contribution at 399.2 eV is given by CoN4 centers, while the one at 400.8 eV comes from the pyrrolic N [12] and most probably from the N+ in pyridinium.[13] The Co2p core-level spectra, unlike the pure **CoTmTPyPz**, shows two photopeaks at 779.1 and 781.2 eV and a shake-up satellite around 785 eV characteristic to 3d7 Co2+. The sharp peak at 779.1 eV could be attributed to a charge transfer to the Co atoms due to the interaction with the substrate surface. Extensive research has been conducted to show the interaction of **CoTmTPyPz** with different conductive substrates, metallic,[12a, 14] or carbon-based.[12a] As a strong interaction of **CoTmTPyPz** with CNT has been proven to exist,[15] it is reasonable to assume that the peak at 779.1 eV comes from it. The contribution at 781.2 eV together with the satellite are probably coming from the bulk **CoTmTPyPz**.[14a] There is a difference between the ratios of the areas of the two types of Co can be explained by an inhomogeneity in the thicknesses of **CoTmTPyPz** layers in the electrode before and after electrolysis. Another possible explanation, given by Muller et al [12a] and supported by the fact that the increase in area of the Co2p3/2 component at 781.2 eV is accompanied by an increase in the area of 400.8 eV component of N1s core-level spectrum of the electrode after catalysis is the disintegration of a small part of CoN4 centers followed by the oxidation of Co atoms. In this case, the Co2p3/2 peak at 781.2 V could be attributed to the Co(II) oxide which, in addition, is accompanied by a satellite located at about 750 eV. The UV/Vis spectra of the **CoTmTPyPz**/CNT/CP electrodes were obtained in solid form both before and after electrolysis. These spectra exhibited comparable reflectance peaks, indicating that the molecules underwent only a minimal decomposition during the electrolysis process (Figure S18).

With the target to relate the impact of the fused pyridinium functions in the **CoTmTPyPz** catalyst, a controlled experiment was conducted with the parent **CoPc**. The **CoPc**/CNT/CP electrode was prepared by dropcasting a **CoPc** solution onto the same CNT/CP electrode precursor under similar concentration.

The **CoPc**/CNT/CP electrode was then subjected to CO_2 electrolysis in CO_2-saturated 0.5 M $KHCO_3$ aqueous solution at -1.0 V *vs*. RHE. The average current density observed for one-hour electrolysis was -18.12 mA.cm^{-2}, a value somewhat lower than that of **CoTmTPyPz**/CNT/CP (Figure 3a). According to the liquid product analysis from ^{1}H NMR, **CoPc** also converts CO_2 to MeOH as already reported with a 6.9% faradaic efficiency under our experimental conditions, which is half of that of **CoTmTPyPz**/CNT/CP (13.8%) (Figure 3b). Furthermore, the partial current density for methanol formation from **CoTmTPyPz**/CNT/CP is three times higher than that of **CoPc**/CNT/CP (Figure S19). These findings suggest that the pyridinium substituents can significantly enhance the methanol formation, likely through a more competent proton and electron transfer to the metal bound CO_2 intermediate.

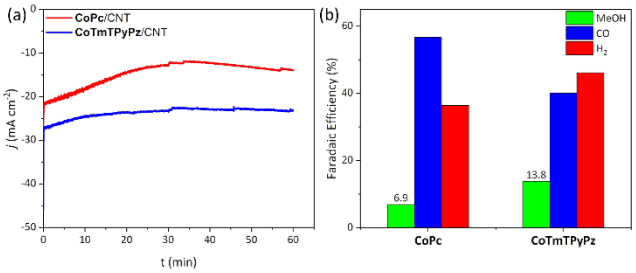

Figure 3. a) current density *vs* t and b) faradaic efficiency of MeOH (green), CO (blue) and H_2 (red) of 1 hour electrolysis of **CoTmTPyPz**/CNT/CP (blue) and **CoPc**/CNT/CP (red) in CO_2-saturated 0.5 M $KHCO_3$ aqueous solution (pH = 7.3) at -1.0 V *vs* RHE.

To gain further insight in the probable mechanistic route how the fused pyridinium functions at the periphery of the porphyrazine core are intervening in the direct CO_2 reduction, we performed an experiment where a pyridinium salt was added to the electrolyte. This approach is based on previous studies as reported by Smith et al. where NADH-like additives were incorporated into the electrolyte of CO_2 electroreduction by iron porphyrin, resulting in a 13-fold increase in the CO production rate.[16] While Zhang et al. modified a cobalt porphyrin by attaching four N-methylpyridinium groups and discovered that CO_2 photocatalysis in water using the modified form cobalt porphyrin achieved 90% CO/H_2 selectivity.[17] The hydrogen evolution reaction (HER) was significantly suppressed due to an active intermediate with a low-spin d^7 Co^{II} center, which poorly matched in forming an effective molecular orbital association with a 1s(H^+) orbital. The electrolysis was realized with the **CoPc**/CNT/CP electrode in a CO_2-saturated 0.5 M $KHCO_3$ with 1 mM N-methyl pyridinium chloride salt. Under these conditions, the current density of **CoPc**/CNT/CP dropped from -13.0 to -10.7 mA.cm^{-2} (Figure S21a). The gas product analysis results suggest that the presence of the pyridinium additive in the electrolyte led to a decrease of the CO selectivity to 29.3 % coupled with an unexpected increase in the H_2 production to 70.7 % (Figure S21b). More importantly, the liquid product analysis from the ^{1}H-NMR of the **CoPc**/CNT/CP modified electrode in 0.5 M KHCO3 aqueous solution with 1 mM pyridinium did not reveal any methanol signal (Figure S22). Hence, these results provide a clear support that the exogeneous pyridinium cannot function the same way as the embarked pyridinium-substituted **CoTmTPyPz** for CO_2 reduction to MeOH. A controlled experiment of formate electrolysis using **CoTmTPyPz** was conducted to investigate if formate could be a potential intermediate. Despite performing a 2-hour electrolysis at the optimal potential of methanol production with 10 mM HCOOH in 0.1 M KHCOO, no methanol was detected in the post-electrolysis electrolyte (Figure S23).

In this report, we have found that fused pyridinium units on the contour of a cobalt pyridinoporphyrazine, **CoTmTPyPz**, when used as a catalyst at a modified **CoTmTPyPz**/CNT/CP electrode could catalytically convert CO_2 to MeOH with a 15% yield under our reported conditions. Interestingly, in contrast with the majority of the reported **CoPc** catalysts where the doubly reduced CO form was found to be the intermediate leading to the formation of MeOH, no such reactivity pattern was observed with the tetracationic **CoTmTPyPz** catalyst. Therefore, insinuating an alternative mechanistic route is undergoing. A further comparative experiment was also undertaken in line with the report from Robert *et col.*, where the authors found an increase in the MeOH formation upon electrolysis of CO in a basic condition. The **CoPc**/CNT/CP electrode was used for electrolysis of CO in a CO-saturated 0.1 M KOH aqueous solution with the presence of 1 mM pyridinium. Here too, like the results obtained from CO_2 electrolysis depicted in Figure S24 and S25, no methanol formation was detected from using CO instead of CO_2. When mixed with an exogeneous source of a pyridinium salt the catalytic performance for the reduction of CO_2 or CO to methanol of **CoPc** was not enhanced. Put together, our results clearly highlight that the covalently integrated pyridinium functionalities on the periphery of the porphyrazine promotes the direct reduction of CO_2 to methanol, where CO is not an apparent intermediate in this multielectron and proton catalytic process. Further investigation on the in-situ study coupled with DFT calculations is under way to interrogate this unique structure/reactivity in the design of molecular catalysts.

Acknowledgements

This work has been supported by the French National Research Agency. We thank CNRS, CEA Saclay, ICMMO and University Paris-Saclay for the financial support. A.A thanks Institut Universitaire de France for financial support. We also thank the analytical support facility at ICMMO for their help with XPS. ASS wants to thank the European Regional Development Fund “A way to make Europe” and the Spanish Ministerio de Ciencia e Innovación/Agencia Estatal de Investigación (PID2020-117855 RB-I00) for funding.

Keywords: carbon dioxide • electrocatalysis • cobalt pyridinoporphyrazine • cobalt phthalocyanine •methanol • biomimetic

Reference

[1] a) M. Bernal, A. Bagger, F. Scholten, I. Sinev, A. Bergmann, M. Ahmadi, J. Rossmeisl, B. R. Cuenya, *Nano Energy* **2018**, *53*, 27-36; b) Y. Y. Birdja, J. Shen, M. T. M. Koper, *Catal. Today* **2017**, *288*, 37-47; c) S. Brandès, V. Quesneau, O. Fonquernie, N. Desbois, V. Blondeau-Patissier, C. P. Gros, *Dalton Trans.* **2019**, *48*, 11651-11662; d) C. Costentin, S. Drouet, M. Robert, J.-M. Savéant, *Science* **2012**, *338*, 90-94; e) P. De La Torre, J. S. Derrick, A. Snider, P. T. Smith, M. Loipersberger, M. Head-Gordon, C. J. Chang, *ACS Catal.* **2022**, *12*, 8484-8493; f) D. Gao, H. Zhou, F. Cai, D. Wang, Y. Hu, B.

Jiang, W.-B. Cai, X. Chen, R. Si, F. Yang, S. Miao, J. Wang, G. Wang, X. Bao, *Nano Res.* **2017**, *10*, 2181-2191; g) S. Gonglach, S. Paul, M. Haas, F. Pillwein, S. S. Sreejith, S. Barman, R. De, S. Müllegger, P. Gerschel, U.-P. Apfel, H. Coskun, A. Aljabour, P. Stadler, W. Schöfberger, S. Roy, *Nature Commun.* **2019**, *10*, 3864; h) Z. Yin, H. Peng, X. Wei, H. Zhou, J. Gong, M. Huai, L. Xiao, G. Wang, J. Lu, L. Zhuang, *Energy Environ. Sci.* **2019**, *12*, 2455-2462; i) X. Zhang, J. Li, Y.-Y. Li, Y. Jung, Y. Kuang, G. Zhu, Y. Liang, H. Dai, *J. Am. Chem. Soc.* **2021**, *143*, 3245-3255.

[2] a) M.-J. Cheng, Y. Kwon, M. Head-Gordon, A. T. Bell, *J. Phys. Chem. C* **2015**, *119*, 21345-21352; b) J. S. Derrick, M. Loipersberger, S. K. Nistanaki, A. V. Rothweiler, M. Head-Gordon, E. M. Nichols, C. J. Chang, *J. Am. Chem. Soc.* **2022**, *144*, 11656-11663; c) P. Gotico, B. Boitrel, R. Guillot, M. Sircoglou, A. Quaranta, Z. Halime, W. Leibl, A. Aukauloo, *Angew. Chem. Int. Ed.* **2019**, *58*, 4504-4509; d) A. Khadhraoui, P. Gotico, B. Boitrel, W. Leibl, Z. Halime, A. Aukauloo, *Chem. Commun.* **2018**, *54*, 11630-11633; e) C. Zhang, P. Gotico, R. Guillot, D. Dragoe, W. Leibl, Z. Halime, A. Aukauloo, *Angew. Chem. Int. Ed.* **2023**, *62*, e202214665.

[3] a) D. Kim, J. Resasco, Y. Yu, A. M. Asiri, P. Yang, *Nature Commun.* **2014**, *5*, 4948; b) Z. Weng, Y. Wu, M. Wang, J. Jiang, K. Yang, S. Huo, X.-F. Wang, Q. Ma, G. W. Brudvig, V. S. Batista, Y. Liang, Z. Feng, H. Wang, *Nature Commun.* **2018**, *9*, 415; c) Z. Weng, J. Jiang, Y. Wu, Z. Wu, X. Guo, K. L. Materna, W. Liu, V. S. Batista, G. W. Brudvig, H. Wang, *J. Am. Chem. Soc.* **2016**, *138*, 8076-8079; d) R. De, S. Gonglach, S. Paul, M. Haas, S. S. Sreejith, P. Gerschel, U.-P. Apfel, T. H. Vuong, J. Rabeah, S. Roy, W. Schöfberger, *Angew. Chem. Int. Ed.* **2020**, *59*, 10527-10534.

[4] a) C. Costentin, M. Robert, J.-M. Savéant, *Acc. Chem. Res.* **2015**, *48*, 2996-3006; b) D. K. Bediako, B. H. Solis, D. K. Dogutan, M. M. Roubelakis, A. G. Maher, C. H. Lee, M. B. Chambers, S. Hammes-Schiffer, D. G. Nocera, *Proc. Natl. Acad. Sci.* **2014**, *111*, 15001-15006; c) M. R. Narouz, P. De La Torre, L. An, C. J. Chang, *Angew. Chem. Int. Ed.* **2022**, *61*, e202207666; d) M. M. Roubelakis, D. K. Bediako, D. K. Dogutan, D. G. Nocera, *J. Porphyr. Phthalocya.* **2021**, *25*, 714-723; e) J. Grodkowski, P. Neta, E. Fujita, A. Mahammed, L. Simkhovich, Z. Gross, *J. Phys. Chem. A* **2002**, *106*, 4772-4778.

[5] a) E. Boutin, M. Wang, J. C. Lin, M. Mesnage, D. Mendoza, B. Lassalle-Kaiser, C. Hahn, T. F. Jaramillo, M. Robert, *Angew. Chem. Int. Ed.* **2019**, *58*, 16172-16176; b) S. Ren, D. Joulié, D. Salvatore, K. Torbensen, M. Wang, M. Robert, C. P. Berlinguette, *Science* **2019**, *365*, 367-369; c) M. Wang, K. Torbensen, D. Salvatore, S. Ren, D. Joulié, F. Dumoulin, D. Mendoza, B. Lassalle-Kaiser, U. Işci, C. P. Berlinguette, M. Robert, *Nature Commun.* **2019**, *10*, 3602; d) Z. Yue, C. Ou, N. Ding, L. Tao, J. Zhao, J. Chen, *ChemCatChem* **2020**, *12*, 6103-6130.

[6] a) C. Zhang, D. Dragoe, F. Brisset, B. Boitrel, B. Lassalle-Kaiser, W. Leibl, Z. Halime, A. Aukauloo, *Green Chem.* **2021**, *23*, 8979-8987; b) X. Zhang, Z. Wu, X. Zhang, L. Li, Y. Li, H. Xu, X. Li, X. Yu, Z. Zhang, Y. Liang, H. Wang, *Nature Commun.* **2017**, *8*, 14675.

[7] a) Y. Wu, G. Hu, C. L. Rooney, G. W. Brudvig, H. Wang, *ChemSusChem* **2020**, *13*, 6296-6299; b) Y. Wu, Z. Jiang, X. Lu, Y. Liang, H. Wang, *Nature* **2019**, *575*, 639-642; c) L. Yao, K. E. Rivera-Cruz, P. M. Zimmerman, N. Singh, C. C. L. McCrory, *ACS Catal.* **2024**, *14*, 366-372; d) J. Shen, R. Kortlever, R. Kas, Y. Y. Birdja, O. Diaz-Morales, Y. Kwon, I. Ledezma-Yanez, K. J. P. Schouten, G. Mul, M. T. M. Koper, *Nature Commun.* **2015**, *6*, 8177; e) Y. Song, P. Guo, T. Ma, J. Su, L. Huang, W. Guo, Y. Liu, G. Li, Y. Xin, Q. Zhang, S. Zhang, H. Shen, X. Feng, D. Yang, J. Tian, S. K. Ravi, B. Z. Tang, R. Ye, *Adv. Mat.* **2024**, *36*, 2310037; f) B. Hu, B. Chu, H. Cao, Z. Lei, S. Cui, P. Wang, J. Tang, X. Wang, B. Xu, *Chem Catal.* **2024**, *4*, 101014.

[8] L.-L. Shi, M. Li, B. You, R.-Z. Liao, *Inorg. Chem.* **2022**, *61*, 16549-16564.

[9] a) H. Rao, L. C. Schmidt, J. Bonin, M. Robert, *Nature* **2017**, *548*, 74-77; b) C. Costentin, M. Robert, J.-M. Savéant, A. Tatin, *Proc. Natl. Acad. Sci.* **2015**, *112*, 6882-6886.

[10] a) T. D. Smith, J. Livorness, H. Taylor, J. R. Pilbrow, G. R. Sinclair, *J. Chem. Soc., Dalton Trans.* **1983**, 1391-1400; b) D. Wöhrle, J. Gitzel, I. Okura, S. Aono, *J. Chem. Soc., Perkin Trans. 2* **1985**, 1171-1178; c) P. Janda, J. Weber, L. Dunsch, A. B. P. Lever, *Anal. Chem.* **1996**, *68*, 960-965; dY. H. Tse, P. Janda, A. B. P. Lever, *Anal. Chem.* **1994**, *66*, 384-390.

[11] N. Heppe, C. Gallenkamp, S. Paul, N. Segura-Salas, N. von Rhein, B. Kaiser, W. Jaegermann, A. Jafari, I. Sergueev, V. Krewald, U. I. Kramm, *Chem. Eur. J.* **2023**, *29*, e202202465.

[12] a) K. Müller, M. Richter, D. Friedrich, I. Paloumpa, U. I. Kramm, D. Schmeißer, *Solid State Ion.* **2012**, *216*, 78-82; b) S. Yu, S. Ahmadi, C. Sun, P. T. Z. Adibi, W. Chow, A. Pietzsch, M. Göthelid, *J. Chem. Phys.* **2012**, *136*, 154703.

[13] M. K. Bayazit, L. O. Pålsson, K. S. Coleman, *RSC Adv.* **2015**, *5*, 36865-36873.

[14] a) F. Petraki, H. Peisert, I. Biswas, T. Chassé, *J. Phys. Chem. C* **2010**, *114*, 17638-17643; b) M. Zhu, J. Chen, R. Guo, J. Xu, X. Fang, Y.-F. Han, *Appl. Catal. B- Environ.* **2019**, *251*, 112-118; c) S. Lindner, U. Treske, M. Knupfer, *Appl. Surf. Sci.* **2013**, *267*, 62-65.

[15] P. O. Krasnov, T. V. Basova, A. Hassan, *Appl. Surf. Sci.* **2018**, *457*, 235-240.

[16] P. T. Smith, S. Weng, C. J. Chang, *Inorg. Chem.* **2020**, *59*, 9270-9278.

[17] X. Zhang, K. Yamauchi, K. Sakai, *ACS Catal.* **2021**, *11*, 10436-10449.

X: @A_Sastre_Santos

Entry for the Table of Contents

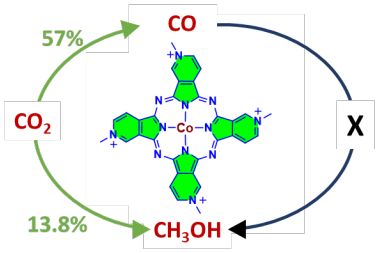

In this study, we investigate the electrocatalytic properties of tetracationic cobalt (II) tetrapyridinoporphyrazine (**CoTmTPyPz**) for CO_2 reduction in a heterogeneous medium when adsorbed on carbon nanotubes (CNT) at a carbon paper (CP) electrode. Unlike previous reports on cobalt-based phthalocyanine electrocatalysis, which suggested CO as an intermediate in the reduction to methanol, our findings indicate that **CoTmTPyPz** does not reduce CO to methanol, thereby excluding a mechanistic pathway where CO is an intermediate.